Enhanced hydrocarbon recovery using the application of seismic attributes in fault detection and direct hydrocarbon indicator in Tomboy Field, western-Offshore Niger Delta Basin

Kelechi N Ibekwe[1], Chinazaekpere Arukwe[2], Chibuzor Ahaneku[2,3], Evangeline Onuigbo[2], Jerry O Omoareghan[1], Ademola Lanisa[1], and Vivian O Oguadinma[1,4]

[1]TotalEnergies SA
[2]Department of Geological Sciences, Nnamdi Azikiwe University
[3]Department of Geosciences, Marine Geology and Seafloor Surveying, University of Malta
[4]UMR 8187, LOG, Laboratoire d'Océanologie et de Géosciences, Univ. Lille, CNRS, Univ. Littoral Côte d'Opale

January 24, 2023

Enhanced hydrocarbon recovery using the application of seismic attributes in fault detection and direct hydrocarbon indicator in Tomboy Field, western-Offshore Niger Delta Basin

Kelechi N. Ibekwe[a*], Chinazaekpere Arukwe[b], Chibuzor Ahaneku[b, d], Evangeline Onuigbo[b], Jerry O. Omoareghan[a], Ademola Lanisa[a], Vivian O. Oguadinma[a, c,]

[a] TotalEnergies SA, CSTJF, Avenue Larribau, Pau 64000, France

[b] Department of Geological Sciences, Nnamdi Azikiwe University, Awka 420007, Nigeria

[c] Univ. Lille, CNRS, Univ. Littoral Côte d'Opale, UMR 8187, LOG, Laboratoire d'Océanologie et de Géosciences, Lille F-59000, France

[d] Marine Geology and Seafloor Surveying, Department of Geosciences, University of Malta, Msida MSD-2080, Malta

*Corresponding author. E-mail address: ibekwekel@gmail.com

Abstract

Seismic stratigraphic and structural interpretation is often hampered by seismic resolution and, sometimes, human's inability to identify a subtle feature on the seismic. These factors have frequently led to the poor seismic interpretation of geologic features. Thus, an integral approach to studying the structural patterns and hydrocarbon bearing zones using seismic attributes were carried out on the Tomboy field using 3D seismic data covering approximately 56 km^2 of the western belt of the Niger Delta. The seismic volume underwent post-stack processing, which enhanced seismic discontinuities. A deep steering volume was first created, and several dip filters were applied to enhance faults in the study area. After that, curvature and similarity attributes were calculated on the dip-steered and fault-enhanced volume. These calculations show detailed geometry of the faults and zones of subtle lineaments. Six faults (F1, F2, F3, F4, F5, and F6) were identified and mapped. These faults range from antithetic to crestal growth faults. Two major growth faults (F5 and F6) were revealed to dip in the NE-SW directions. A near-extensive crestal fault (F4) appeared beneath the major faults. Although several minor fractures were displayed in the southern and central portion of the seismic data, the SW dipping crestal fault (F4) and growth fault F6 are responsible for holding the hydrocarbon found within the identified closures. Using attributes on the seismic data increased confidence in the mapping and interpreting structural features. Furthermore, Energy attributes were used as Direct Hydrocarbon Indicator (DHI) to visualize viable areas within the study and permits a more robust interpretation. Time slices were taken at regions of flat and bright spots. Spectral decomposition attribute was run on these slices to display areas of high amplitude reflection typical of hydrocarbon-bearing regions, which are trapped mainly by regional to sub-regional growth faults. The surface attribute calculated on the generated surface shows that the field is dominantly controlled by faults serving as traps for hydrocarbon.

Keywords: Seismic attributes; Niger Delta Basin; Faults; Bright spots

1. Introduction

The seismic attributes used in studies are suggested to be all the information obtained from seismic data, either by direct measurements or logical or experience-based reasoning (Taner, 2001; Thapar, 2004). Chopra and Marfurt (2005) defined seismic attributes as any information derived from seismic data, such as interval velocity, inversion for acoustic impedance, pore pressure prediction, and reflector terminations. Seismic attribute analysis has also been a vital aid in seismic interpretation since 1930 when geophysicists discovered the first seismic section. Ever since more than 50 attributes of seismic data have been obtained, more types of attributes have been found with the advance in computer technology. For reservoir characterisation (Lunina et al., 2014; Shang et al., 2022) and seismic interpretations, seismic attributes analysis has been used by many authors (Vetrici and Stewart, 1996; Strecker et al., 2004; Ajisafe and Ako, 2013; Oguadinma et al., 2016; Oguadinma et al., 2021). It also proved its importance in the classification of the depositional environment (Ahmad and Rowel, 2013; Matos and Marfurt, 2013) and the detection and enhancement of fractures and faults (Ayolabi and Adigun, 2013; Castillo, 2010; Francelino and Antunes, 2013; Santosh et al., 2013) to give details of structural history and to provide direct hydrocarbon indicator (Adepoju et al., 2013). The seismic attribute technique is often used in seismic data processing because it can enhance geological information not observed using the conventional processing method (Ayolabi and Adigun, 2013). Chopra (2002) used similarity as a coherence attribute in detecting trace discontinuities of the seismic data to detect faults and stratigraphic features. The curvature attribute is used in 3D horizon interpretation to characterize faults and fracture systems (Robert, 2001). In 3D seismic data volume, fault dipping can be detected using a semblance-based coherency algorithm (Marfurt et al., 1998, 1999). The study of Jones and Roden (2012) used the geometry seismic attribute technique of dip of maximum similarity and curvature types in investigating the fault system of the South Texas oil field. Their study showed that the geometry seismic attribute technique helped enhance and detect faults and fractures. At the same time, the curvature attributes were also applied to highlight other features not revealed by the geometry attributes application. This paper sets out to enhance fault visualisation and highlight viable hydrocarbon placement using seismic attributes in the study area in the Niger Delta Basin.

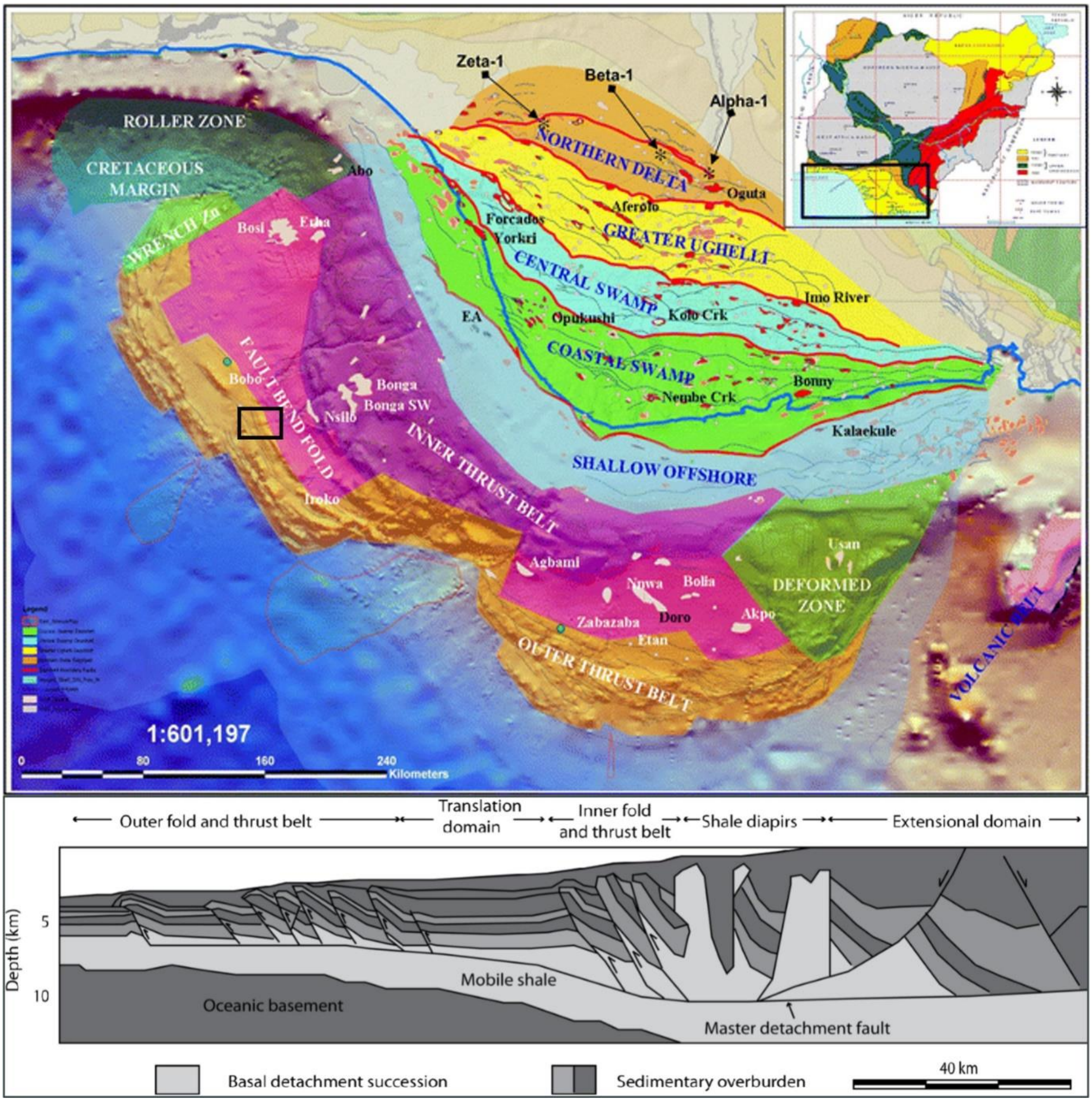

Fig. 1. *(a) The Niger Delta complex showing different depocenters and the location of the studied area in a black box (modified from Ejedawe et al., 2002). (b) Cross-section through the Niger Delta showing the gross architecture and structural style typical of large deltas situated on passive margins (Corredor et al., 2005).*

2. Geologic background

Tomboy field is located in the offshore western Niger Delta Basin (Fig. 1). This basin is situated in the Gulf of Guinea, Central Africa. It lies between latitudes 4° and 6°N and longitudes 3° and 9°E. A regressive sequence where the rate of sediment supply is higher than the subsidence rate (Reijers, 2011) causes the accumulation of clastic wedges approximately 12 km thick in the basin. It has been documented that the tectonic framework of the Niger Delta margin along the western coast is controlled by Cretaceous fracture zones that appear as ridges and sometimes trenches in the deep part of the Atlantic Ocean (Lehner and Ruiter, 1977).

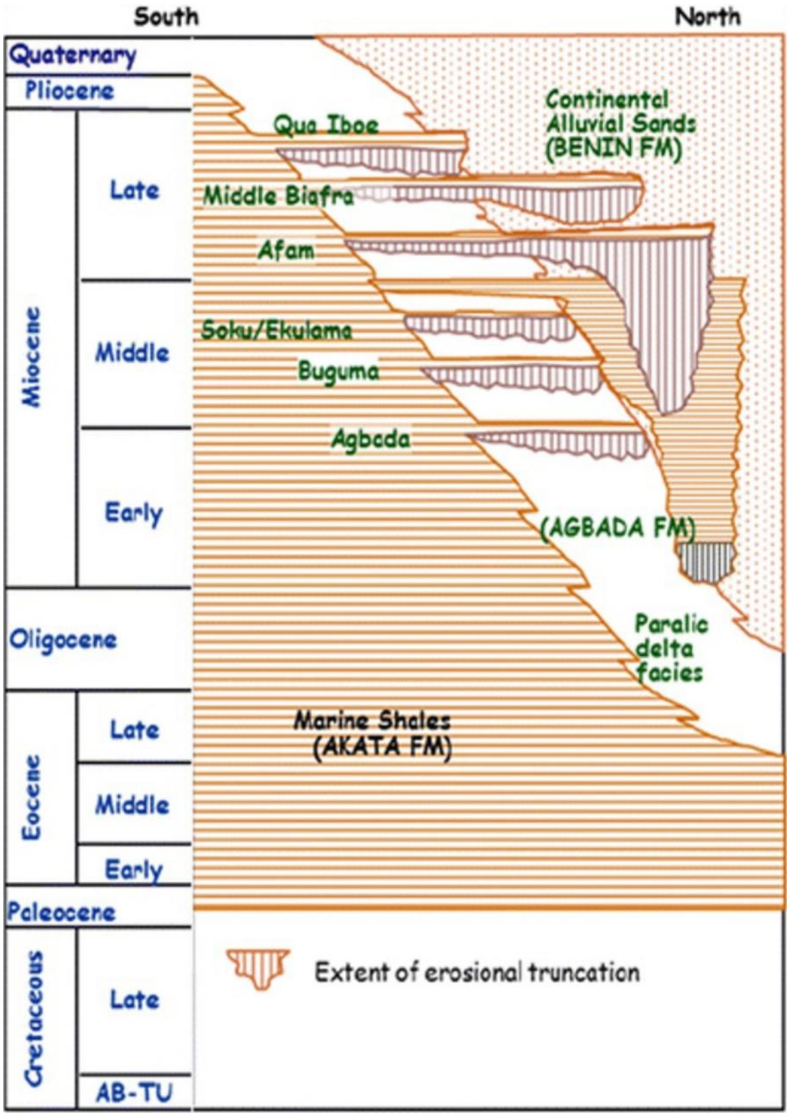

Fig. 2. *Regional stratigraphy of the Niger Delta showing different geologic formations (Akata Formation, which is the oldest; Agbada Formation that overlies the Akata and the youngest Benin Formation containing mainly alluvial deposits) (Ozumba, 2013).*

In the delta, shale tectonic activities are on the rise. For instance, shale mobility induced internal deformation in response to some processes. One of the processes is shale diapirism formed from loading poorly compacted and overpressure prodelta and delta slope clay (Agbada Formation; Tuttle et al., 1999) by high-density delta front sands of the Agbada Formation. Another process is slope instability due to a lack of lateral, basin-ward support for the under-compacted delta-slope clay (Akata Formation). The Benin Formation is Oligocene and younger. It comprises continental floodplain sands and alluvial deposits with an estimated 2 km thick deposits (Tuttle et al., 2015). The stratigraphic column of the Niger Delta lithostratigraphic units is shown in Fig. 2.

3. Methodology

This study used 3D seismic data loaded into the OpendTect and Petrel interpretative software. The data was quality-checked for errors, and corrections were made. Before interpretation in Petrel, seismic data was loaded. The data was scanned and realised to improve the signal-to-noise ratio and to decrease the data size so that the data processing and interpretation would be improved. Fault mapping was carried out on the seismic inline and crossline sections manually. The seismic data was steered for a more detailed interpretation, and the objective was to improve the signal-to-noise ratio for better seismic data to run interpretations on.

Seismic attributes such as curvature, semblance, energy and spectral decomposition were used for fault detection and DHI. The similarity attribute has been defined as the Euclidean distance between vectors normalized over the vector lengths. Similarities of one and zero indicate that the trace segments are identical and non-identical, respectively (Tingdahl and De Groot, 2003). Using the OpendTect software window environment, it is observed that the calculation of similarity is often favoured by determining the direction of the best match at every position, which is a result by itself: the dip. Applying the similarity attribute is relatively easy and gives clarity at every stage. When integrated with other attributes, this attribute would most certainly give impressive results in the shortest time possible.

The Spectral decomposition and the semblance attributes maps are based on "horizons" (+/- a few meters around the interpreted horizons). The spectral decomposition RGB frequencies of the blending used were from frequency evaluation of the interval of interest of the seismic data using the work of Peyton et al. (1998). The semblance attribute stresses seismic trace by trace and utilizes observations and interpretations of structural and stratigraphic features.

Different steering cubes were calculated from a different algorithm. From Fig. 3, subtle features in the full stack steering cube were visible after the background steering cube was calculated (Fig. 3c). This region is circled in red. To explain further, dip Steering is used when seismic reflectors are followed by auto-tracking the pre-calculated dip field from any starting position. Working with more than a steering cube is essential hence the three steering cubes in this study: the Full steering cube, the Detailed steering cube and the Background steering cube.

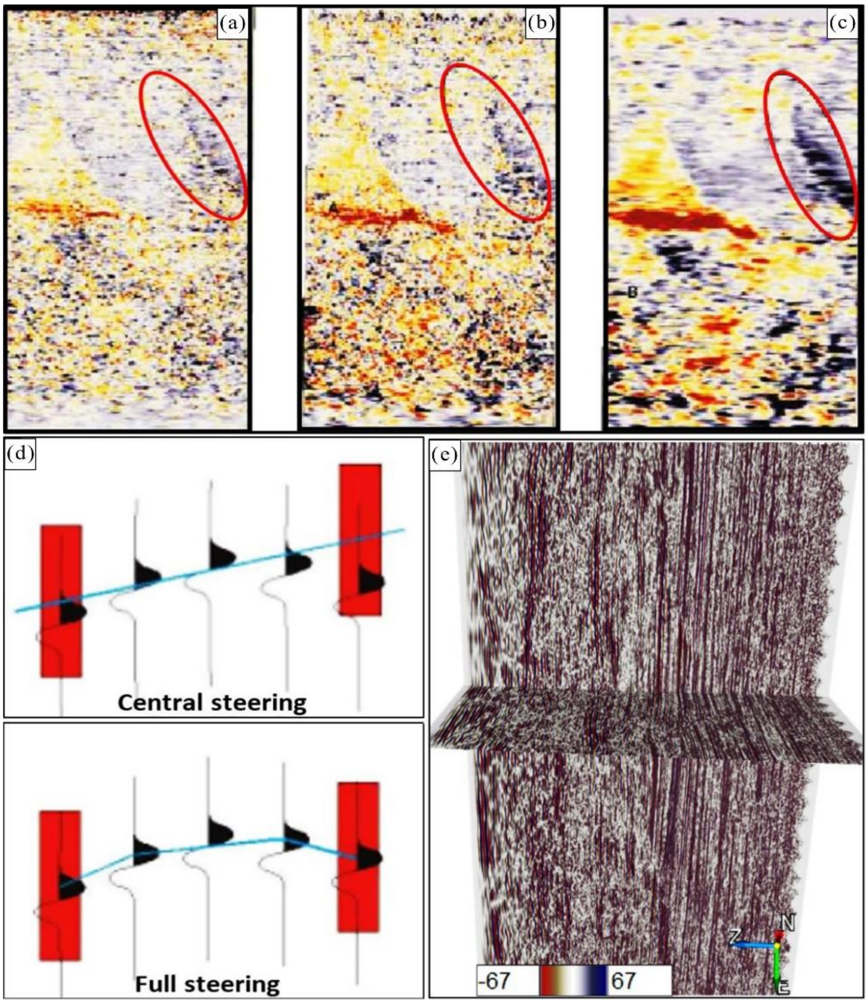

Fig. 3. *(a) Full stack steering cube, (b) Detailed steering cube and (c) background steering cube. Notice how the fault on the full stack steering cube was enhanced at the background steered cube. (d) Comparison between central and full steering cube. It appears that the relationship in the full steering cube is better than the centre while the detailed and background steering are better than the full steering cube. (e) Seismic survey base map of the study area displaying seismic inline and cross line. The red box represents the location of the study area.*

In OpendTect, data-driven steering is of two types: Central and Full steering (Fig. 3d). Where Central steering dip/azimuth at the point of evaluation point is followed by trace segment to compute filters and seismic trace at an event, the Full steering, at every tract position, is updated. The Detailed steering cube is made of dips calculated from the dip-computation algorithm and is used to preserve details in the data (Fig. 3 and Table 1). For example, in a fracture detection study. On the other hand, the Background steering cube is usually median-filtered and a smoothed version of the Detailed steering cube. If well filtered, it contains less noise; notably, the dips follow larger structural trends.

Table 1 *Settings of seismic attributes with values of dip-steered attribute, step-out, satistical operator and time gate.*

Attribute	Dip-steering	Step-out	Statistical operator	Time gate (ms)
Similarity	Not steered	N/A	Minimum	(-24, 24)
Curvature	Steered	(1, 1, 1)	Maximum	(-24, 24)
Raw steering	N/A	(1, 1, 1)	N/A	N/A
Detailed steering	N/A	(1, 1, 3)	N/A	N/A
Background steering	N/A	(5, 5, 0)	N/A	N/A

4. Results and discussion

4.1. Fault interpretation

The structural framework was carried out by picking assigned fault segments on inline 5860, 5884 and 5980 sections of the seismic volume (Figs. 4 and 5).

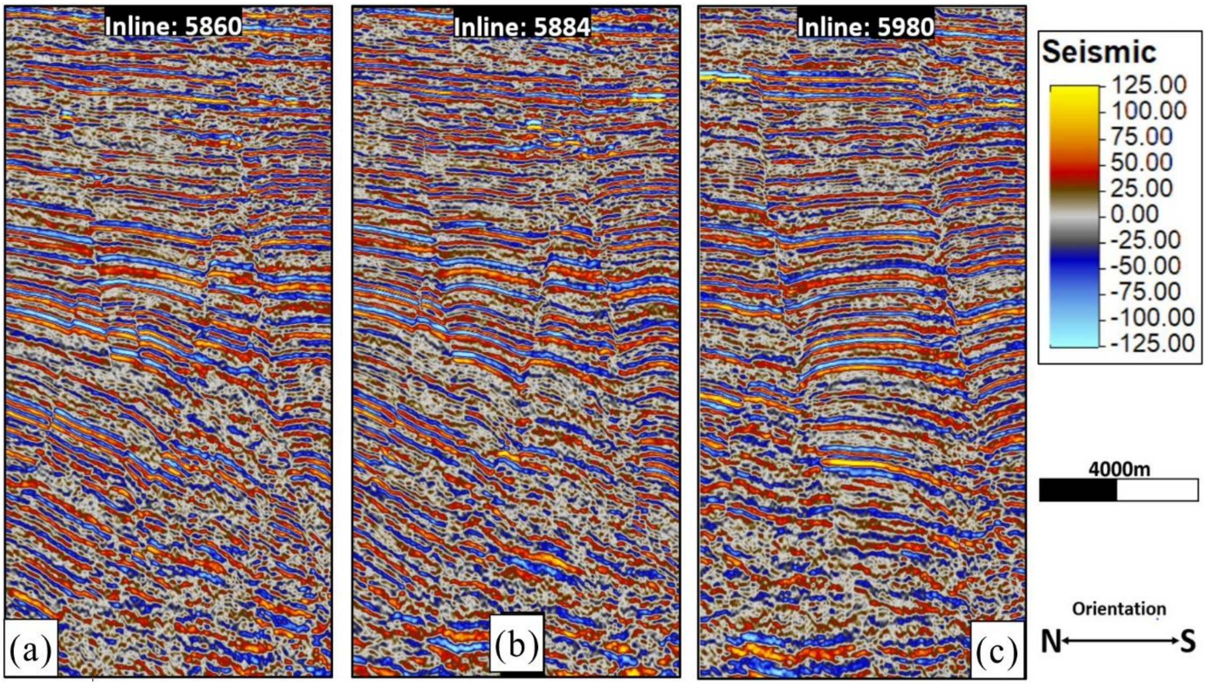

Fig. 4. *Uninterpreted seismic sections of in-lines 5860, 5884, and 5980. Notice the map's legend, scale and orientation on the right-hand side of the figure. #*

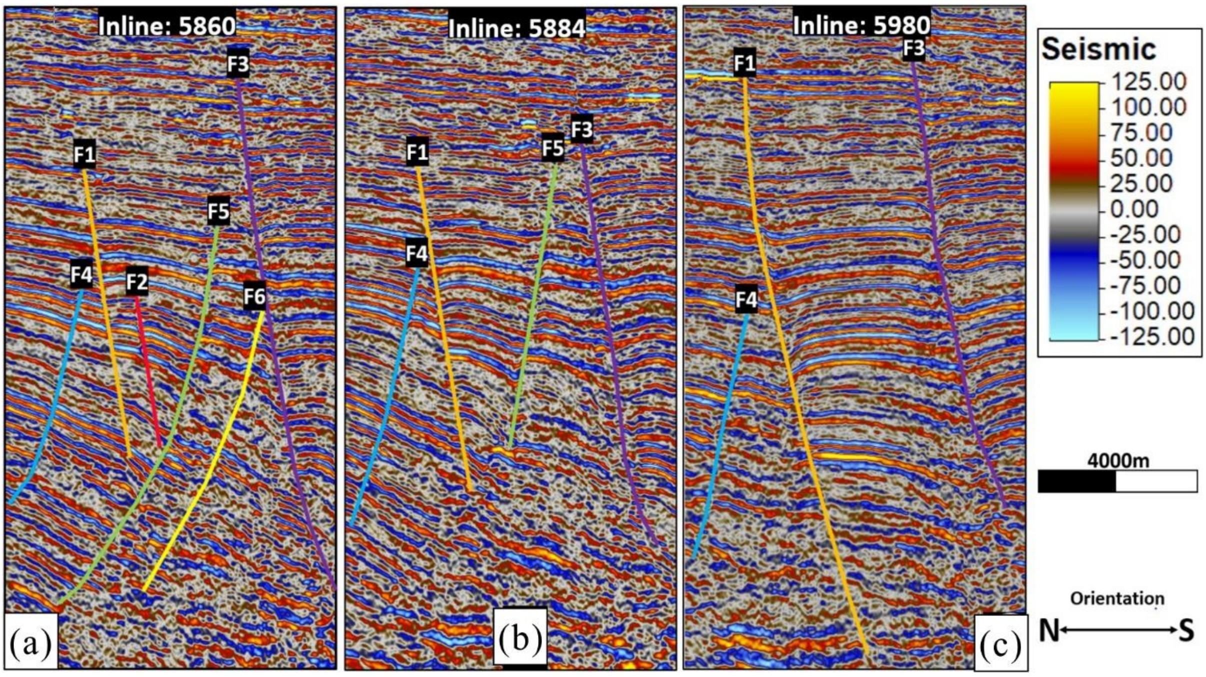

Fig. 5. *Interpretated seismic sections of in-lines 5860, 5884, and 5980. Six faults were observed and interpreted on seismic sections A, B and C.*

These identified and interpreted faults on the seismic sections were due to discontinuous reflection along the disorientation of reflectors or as distortion caused by an anomaly of the amplitude around the fault zones (Ning et al., 2022). A total of six faults noted as F1, F2, F3, F4, F5, and F6 were identified on the inline sections (Figs. 4 and 5; Table 2). Some of these faults extend through the extent of the field, known as major regional growth faults and a few antithetic faults (Table 2). The four growth faults, F1, F3, F5 and F6, are dipping southward, while others dip towards the north except for the minor fault (F2) dipping southwest.

Table 2 *Interpreted faults along the inline sections of the entire 3-D seismic volume noting fault type, dip direction and fault symbols.*

Fault Type	*Dip Direction*	*Fault Symbol*
F1	Southwest	Minor Growth Fault
F2	Southwest	Minor Fault
F3	Southwest	Major Regional Growth Fault
F4	North	Antithetic Fault
F5	Southeast	Major Growth Fault
F6	Northeast	Major Growth Fault

4.2. Attribute analysis and its significance

Different attributes (i.e., similarity, spectral decomposition, energy, and diffusion filter; Table 1) were run on the seismic cube. Z-slices were taken on the original seismic and displayed as flattened maps. Structures respond to acoustic waves differently; thus, the attributes extracted are best used to study different subtle and sub-seismic faults missed by conventional seismic interpretation. Figs. 6 and 7 show the results of similarity attributes applied to the data used for this study and the clarity of structural features it provides. Observe the uninterpreted and interpreted maps from seismic inlines 5884 and 5980. It made subtle features visible and interpretation easy while increasing the results' confidence (Fig. 7).

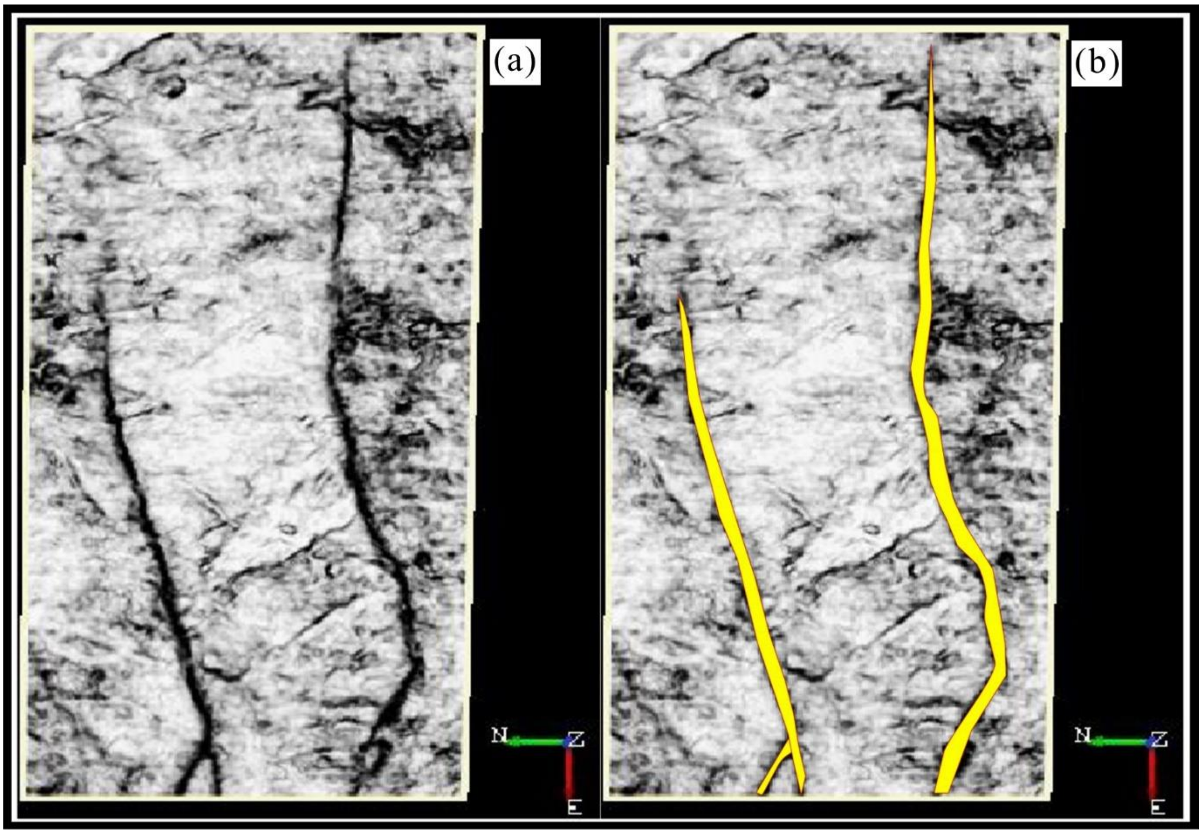

Fig. 6. *Extracted similarity attribute maps from inline 5860. (a) shows the uninterpreted map with regions of possible discontinuous reflections. (b) shows the same map with the interpreted faults.*

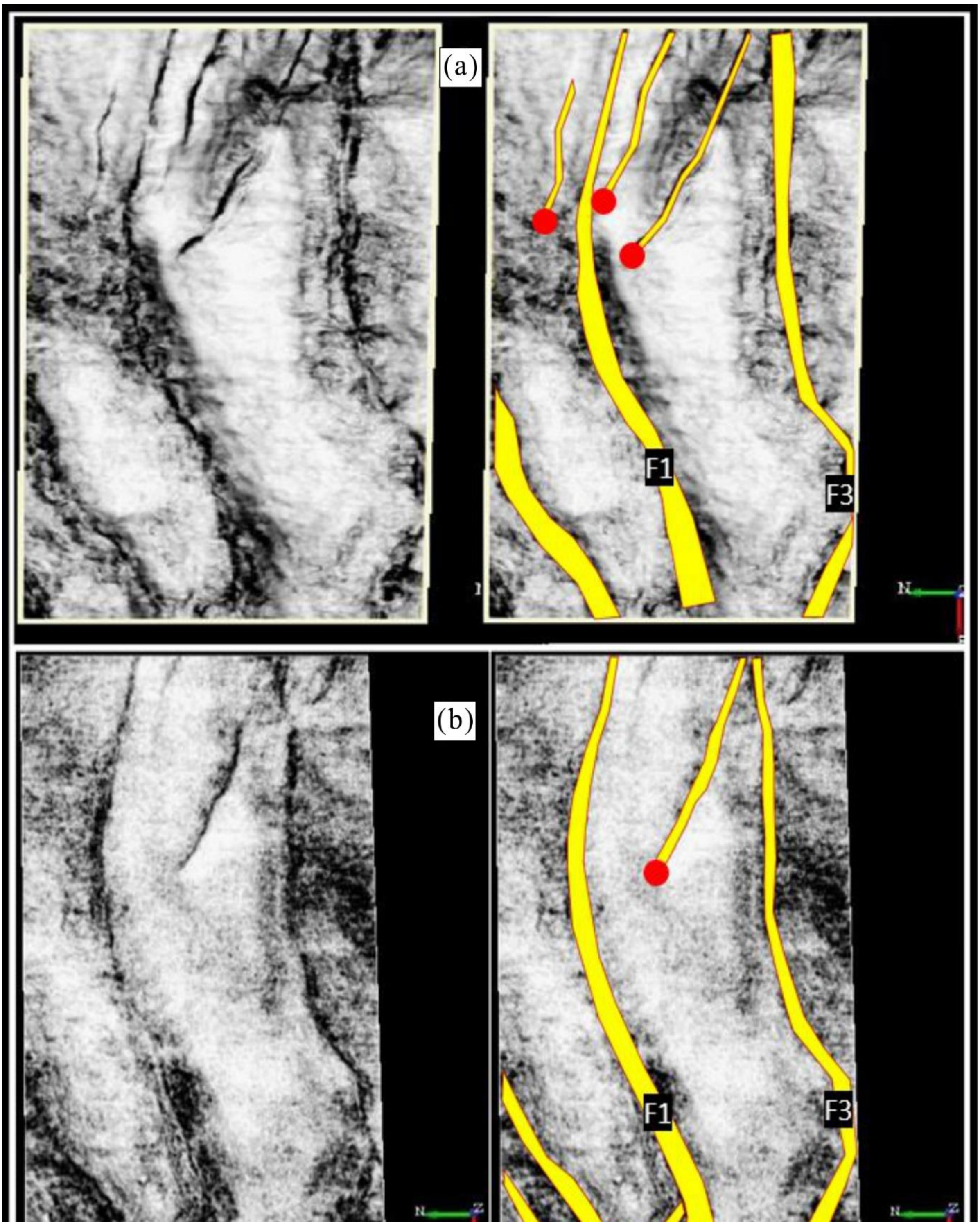

Fig. 7. *Extracted similarity attribute maps from inlines 5884 and 5980. On the left of both (a) and (b) are the uninterpreted maps showing regions of possible discontinuous reflections. On the right are the same map with the interpreted faults. F1 and F3 represent fault one and fault three, respectively. The red circles are placed on faults not identified on the seismic sections.*

The energy attribute is the sum of amplitudes squared in a time gate. It highlights packages with different reflection strengths in seismic reflections (Fig. 10). In siliciclastic, energy attributes can decipher lithology and sediment porosity types and enhance bright spot regions. In this study, the application of energy attribute has made it possible to identify bright spots on the time slices obtained from the seismic volume (see Figs. 8 and 10b), serving as a pre-plan methodology for highlighting possible hydrocarbon regions for good interpretation decisions even without the presence of well logs like gamma-ray and resistivity to help identify and classify reservoir bearing formations. Hence, its usefulness cannot be overemphasized. The application of energy attributes is not universally known, and most researchers and industry experts are oblivious to its use. This is because applying root mean square attribute and spectral decomposition serves similar purposes. However, from the quality of the results generated in this study, the energy attribute has proven to be an even better direct hydrocarbon indicator (DHI) tool for effectively identifying leads and hydrocarbon prospective regions.

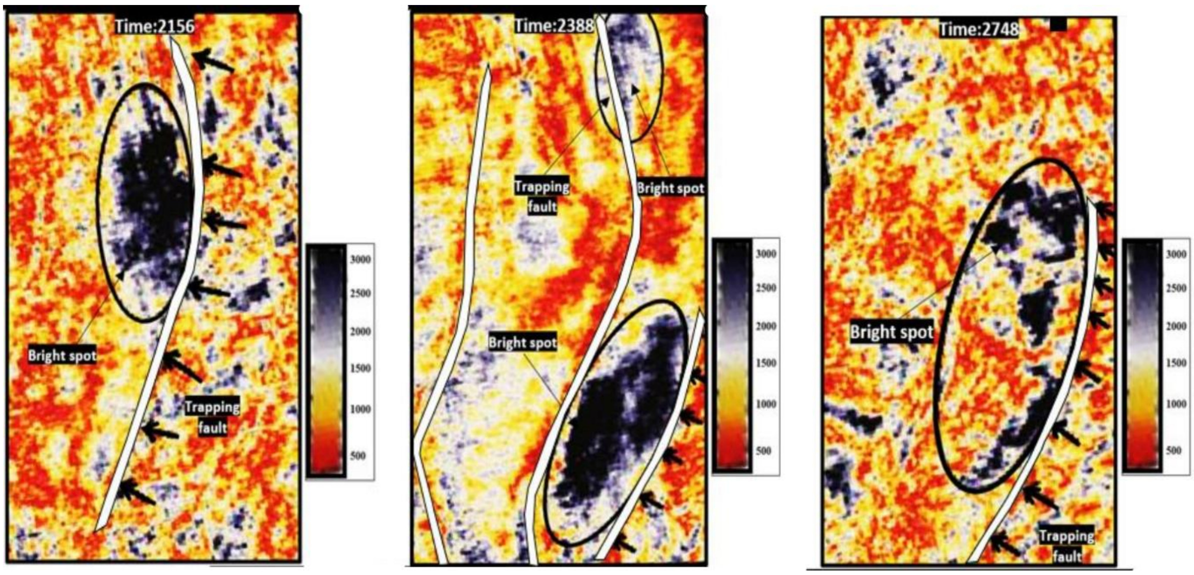

Fig. 8. *Time slices showing areas of high amplitude anomalies observed at times 2156, 2388 and 2748, respectively. Using energy attributes, these areas are interpreted as bright spots (potential hydrocarbon areas), and hydrocarbon accumulation was observed to close up on faults.*

By using the spectral decomposition attribute, the effect of frequency assessment was carried out on the seismic data obtained from the Tomboy field. Observations were made to confirm the viability of the energy attribute application and to ground truth the finding about the field having places of bright spots (Fig. 9b). Firstly, a horizon was interpreted in both the inline and the crossline section across the entire 3D seismic volume. The interpreted horizon is further converted into a time surface map before applying the spectral decomposition attribute (Welsh et al., 2008). The spectral RGB (Red, Green, and Blue) frequencies were fine-tuned to agree with the layer of the horizon that it is to be applied. This action helped manage the frequency difference until the desired output map was clear enough for interpretation to be obtained. Fig. 9a shows a time surface map from time 2388, and Fig. 9b shows the result of the spectral decomposition attribute extracted from the horizon. Notice the abnormally high-frequency reading in the red circle bounded by two faults.

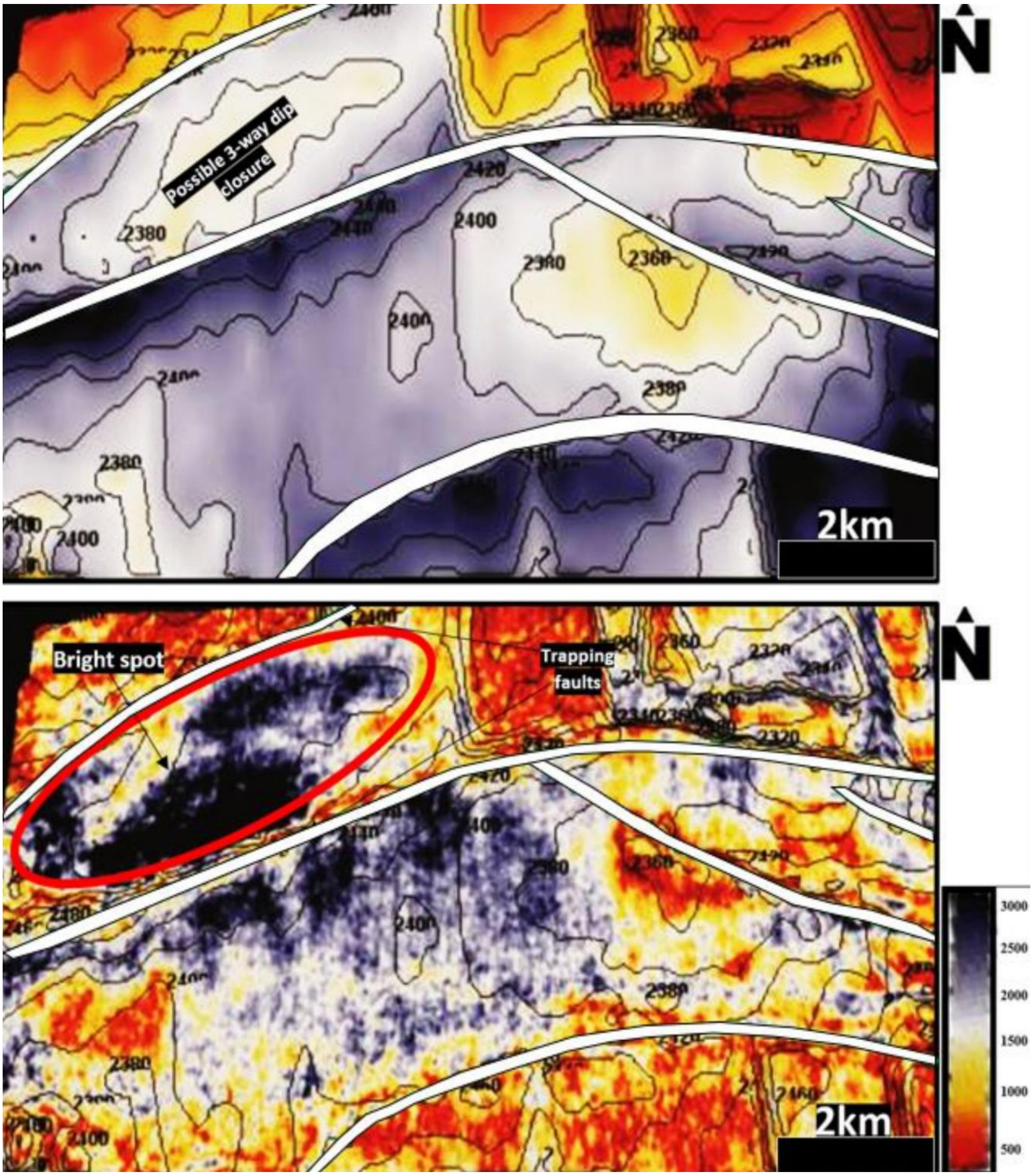

Fig. 9. *(a) Time surface map of a horizon mapped at time 2388 with a series of faults dipping in the SW-NE direction. (b) The spectral decomposition map extracted from the OpendTect software. It shows a bright spot region enclosed in a red circle, closing against faults.*

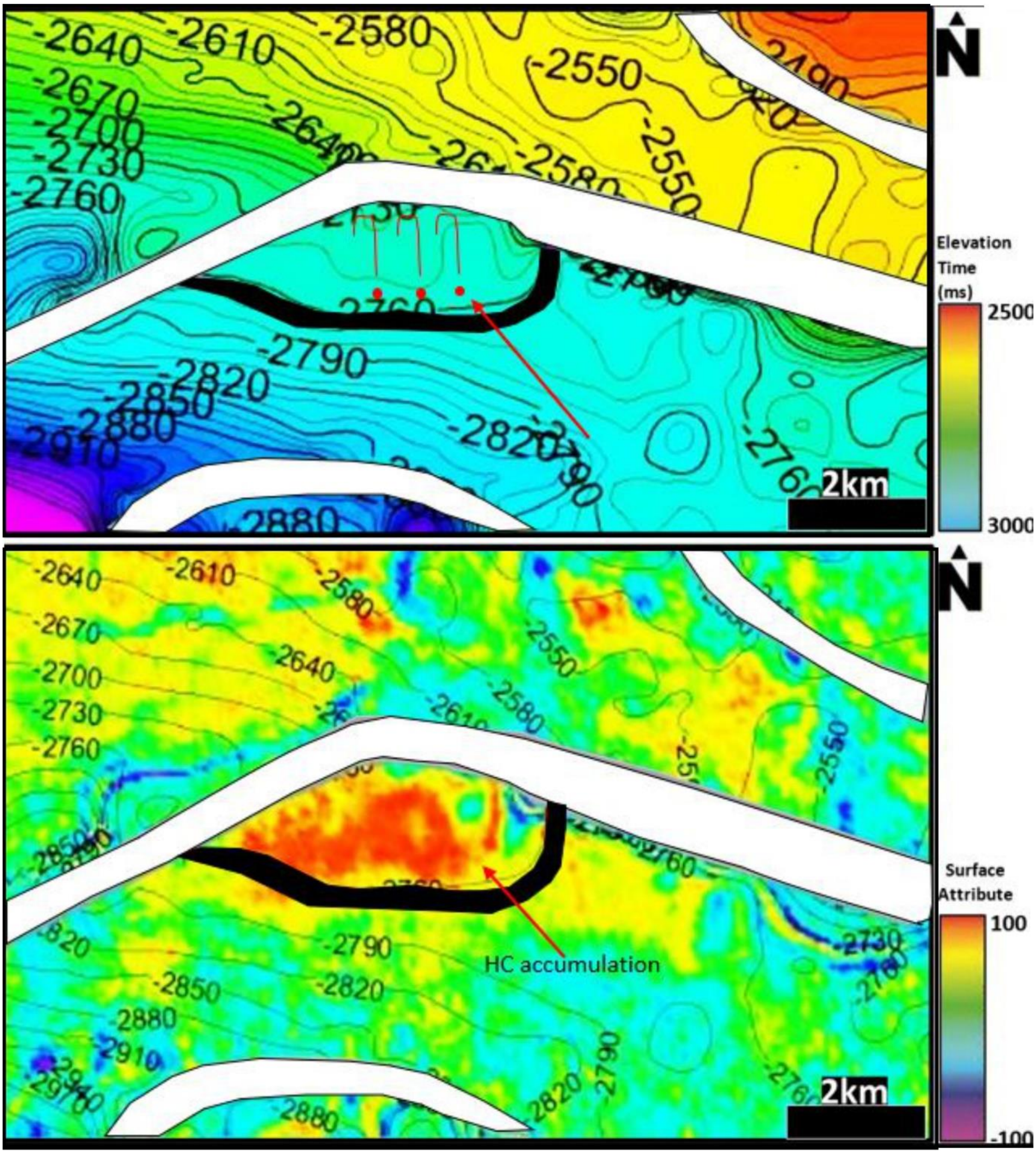

Fig. 10. *(a) Interpreted time surface map of a horizon mapped at 2748 showing faults. (b) Contour 2760 is closing on a major fault. The hydrocarbon-bearing region was evident on this attribute map in contour 2760 of the surface map in (a). HC stands for hydrocarbon accumulation.*

5. Conclusions

Similarity attribute is a great tool for structural interpretation enhancement, and it plays a crucial role in subtle feature detections that would not usually be detected by human eyes or subtle features beyond seismic resolution. These seismic attributes are better applied on horizon and time slices. However, it is advised that data quality checking and signal-to-noise ratio be applied before running the attribute method on the data. This will guarantee a better output of expected results from the data. Interpretation of the 3D seismic data for locating both seismic scales and sub-seismic scale structural elements and areas of possible hydrocarbon accumulation has been demonstrated to be more efficient by using seismic attribute mapping and analysis. From this study, several observations have been made:

- Seismic attributes can be run on an entire 3D seismic volume before interpretation commences.
- Seismic attributes extracted from time slices are essential and can be used as reconnaissance for better visualisation of areas to focus on during a detailed interpretation.
- Spectral decomposition and Energy attributes have proven very useful as direct hydrocarbon indicators by identifying bright spot areas that are interpreted to contain a significant amount of hydrocarbon.
- It was also observed that fault block displacement leads to seismic reflection discontinuity. By identifying and interpreting faults in data, displaced seismic reflections can be better correlated from one fault block to the other. This will enhance interpretation confidence and produce a better result.

Integrated discontinuous attributes and other seismic attributes would yield better hydrocarbon exploration outcomes. Therefore, seismic attribute analysis should be integrated into the standard practice of hydrocarbon exploration and production; and oil companies can quickly reduce the risk of drilling dry holes resulting from missed faults due to conventional seismic interpretation methods.

References

Adepoju, O., Joseph, O., Chukwuemeka, N., 2013. DHI analysis using seismic frequency attribute on field-AN Niger Delta, Nigeria, IOSR Journal of Applied Geology and Geophysics, 1(1), 5–10

Ahmad, M. N., and P. Rowell, 2013. Detection of fluvial sand systems using seismic attributes and continuous wavelet transform spectral decomposition: a case study from the Gulf of Thailand, Mar Geophys Res, Springer.

Ajisafe, Y.C., and B. D. Ako, 2013. 3-D Seismic Attributes for Reservoir Characterization of "Y" Field Niger Delta, Nigeria, IOSR Journal of Applied Geology and Geophysics, 1(2), 23-31.

Ayolabi, E. A., and A. O. Adigun, 2013. The Use of Seismic Attributes to Enhance Structural Interpretation of Z-Field, Onshore Niger Delta, Earth Science Research, 2(2), Canadian Center of Science and Education.

Castillo, F., 2010. Seismic attributes for 3-D fracture interpretation, Halliburton, Geo Canada.

Chopra, S., 2002. Coherence cube and beyond, EAGE First break, 20, 27-33.

Chopra, S., and K. J. Marfurt, 2005. Seismic attributes- A historical perspective, Geophysics, 70 (5).

Corredor et al., 2005. Structural styles in the deep-water fold and thrust belts of the Niger Delta. American Association of Petroleum Geologists Bulletin. 89, 753–780.

Ejedawe J, Fatumbi A, Ladipo K, Stone K., 2002. Pan—Nigeria exploration well look—back (Post-Drill Well Analysis). Shell Petroleum Development Company of Nigeria Exploration Report 2002.

Evamy, B.D., Haremboure, J., Karmerlimg, P., 1978. Hydrocarbon Habitat of Tertiary Niger Delta. American Association of Petroleum Geologists Bulletin, 62, 1-39.

Francelino, A. V. M., and Antunes, A. F., 2013. Applying filters and seismic attributes for enhancing faults in the 3D seismic survey of Alto De Siririzinho (Sergipe-Alagoas Basin, northeast Brazil), Revista Brasileira de geodesic, 31(1), 109-123.

Jones, G. and Roden, R., 2012. Fracture detection interpretation beyond conventional seismic approaches: Presented at AAPG conference.

Lehner, P. and De Ruiter, P. A. C., 1977. Structural history of the Atlantic margin of Africa Am. Assoc. Petrol. Geol. Bull. 61, 961-981

Lunina, O. V., Caputo, R., and Gladkov, A. S., 2014. Southern East Siberia Pliocenee-Quaternary faults Database, analysis and inference. Geoscience Frontiers 5 (2014) 605-619

Marfurt, J., Kirlin, R., Farmer, L., Bahorich, S., 1998. 3-D seismic attributes using a semblance-based coherency algorithm, Geophysics, 63, 1150–1165.

Marfurt, J., Sudhaker, V., Gersztenkorn, A., Crawford, D., Nissen, E., 1999. Coherency calculations in the presence of structural dip, Geophysics, 64, 104–111.

Matos, M. C. D., and K. J. Marfurt, 2013. Subsurface geometry interpretation by integrating continuous wavelet transform seismic attributes," Sismo research and consulting, The University of Oklahoma, 13th international congress of the Brazillian geophysical society.

Ning, F., Yun, J., Zhang, Z., Li, P., 2022. Deformation patterns and hydrocarbon potential related to intracratonic strike-slip fault systems in the east of the Central Uplift Belt in the Tarim Basin. Energy Geoscience 3 (2022) 63-72

Oguadinma, V., Okoro, A., Reynaud, J., Evangeline, O., Ahaneku, C., Emmanuel, A., Eliseus, A., 2021. The art of integration: A basic tool in effective hydrocarbon field appraisal. Mediterranean Geosciences Union Annual Meeting

Oguadinma, V., Nnaemeka, O., Kingsley, E., (2016). An integrated approach to hydrocarbon prospect evaluation of the Vin field, Nova Scotia Basin, Canada. Paper presented at the 2016 SEG International Exposition and Annual Meeting, Dallas, Texas, 99–110.

Ozumba, B., 2013. Geology of the Niger Delta: An Overview for Geophysics Processors. An SPDC presentation for geologists in Nigeria.

Peyton, L., 1998. Interpretation of incised valleys using new 3D seismic techniques: A case history using spectral decomposition and Coherency: *The Leading Edge*, v. 17, p. 1294-1298.

Reijers, T.J.A., 2011. Stratigraphy and Sedimentology of the Niger Delta. Geologos, 17, 133-162. https://doi.org/10.2478/v10118-011-0008-3

Roberts, A., 2001. Curvature attributes and their application to 3D interpreted horizons, First Break, 18, 85-99.

Santosh, D., Aditi, B., Poonam, K., Priyanka S., Rao P.H, Hasan, S. Z., Harinarayana, T., 2013. An Integrated Approach for faults and fractures delineation with dip and curvature attributes, 10th Biennial International Conference & Exposition, Kochi.

Shang, X., Hou, J., Dong, Y., 2022. The genesis of reservoir heterogeneity and its impacts on petroleum exploitation in beach-bar sandstone reservoirs: A case study from the Bohai Bay Basin, China. Energy Geoscience 3 (2022) 35-48

Taner, M. T., 2001. Seismic attribute, CSEG Recorder, 48-56.

Thapar, M. R., 2004. Seismic attributes; Principal & application, Petro Skills, 73–123.

Tingdahl K.M. and de Groot P.F.M., 2003. Post-stack dip- and azimuth processing. Journal of Seismic Exploration 12, 113–126.

Tuttle, M. L. W., Charpentier, R. R., Brownfield, M. E., 2015. The Niger Delta Petroleum System: Niger Delta Province, Nigeria, Cameroon, and Equatorial Guinea, Africa. United States Geologic Survey.

Vetrici, D. G., and Stewart, R. R., 1996. 3-D seismic attributes, CREWS research report, 8(45), 1–30

Welsh, A., Brouwer, F. G. C., Wever, A., 2008. The Spectral decomposition of seismic reflection data to detect Gas related frequency anomalies. 70th EAGE Conference & Exhibition, June 2008, Rome.